Estimating the Time-To-First-Fix for GNSS Signals Theory and Simulation Results

Marco Anghileri, Matteo Paonni, Stefan Wallner, José-Ángel Ávila-Rodríguez, Bernd Eissfeller
Institute of Geodesy and Navigation, University FAF Munich, Germany
marco.anghileri@unibw.de

BIOGRAPHIES

Marco Anghileri is research associate and Ph.D. candidate at the Institute of Geodesy and Navigation at the University FAF Munich. He studied at the Politecnico di Milano, Italy and at the Technical University Munich, Germany and has an MSc in Telecommunication Engineering. His scientific research work focuses on GNSS signal structure and on signal processing algorithms for GNSS receivers.

Matteo Paonni is research associate at the Institute of Geodesy and Navigation at the University of the Federal Armed Forces Munich. He received his M.S. in Electrical Engineering from the University of Perugia, Italy. He is currently involved in several ESA and EC/GSA projects with focus on GNSS. His main topics of interest are GNSS signal structure, GNSS interoperability and compatibility and GNSS performance assessment.

Stefan Wallner studied at the Technical University of Munich and graduated in 2003 with a Diploma in Techno-Mathematics. He is now research associate at the Institute of Geodesy and Navigation at the University of the Federal Armed Forces Germany in Munich. His main topics of interests can be denoted as the Spreading Codes, the Signal Structure of Galileo together with Radio Frequency Compatibility of GNSS.

José Ángel Ávila Rodríguez is research associate at the Institute of Geodesy and Navigation at the University of the Federal Armed Forces Munich. He is responsible for research activities on GNSS signals. Avila-Rodriguez is one of the CBOC inventors and has actively participated in the developing innovations of the CBOC multiplexing. He is involved in the Galileo program, supporting the European Space Agency, the European Commission, and the GNSS Supervisor Authority, through the Galileo Signal Task Force.

Bernd Eissfeller is Full Professor of Navigation and Director of the Institute of Geodesy and Navigation at the University FAF Munich. He is responsible for teaching and research in navigation and signal processing. Till the end of 1993 he worked in industry as a project manager on the development of GPS/INS navigation systems. He received the Habilitation (venia legendi) in Navigation and Physical Geodesy in 1996 and from 1994-2000 he was head of the GNSS Laboratory of the Institute of Geodesy and Navigation.

ABSTRACT

In a constantly evolving GNSS scenario new signals are coming into play for the benefit of the final users, who are more and more interested in understanding the performance differences of the various possibilities they can use. Among the major figures of merit to compare the signals, the Time-to-First-fix (TTFF) plays a very important role. In this paper a methodology for the estimation of the TTFF of various GPS and Galileo signals is presented. The followed approach can be seen as an extension of [1], where the results are computed for a confidence level of 95%. As we all know, most of the time needed to calculate the first fix is spent for the acquisition process and to read the navigation data (satellite ephemeris and clock corrections) for the calculation of the pseudoranges to the satellite. For this reason our work focuses mainly on these two aspects.

Concerning the acquisition, the estimation of the time needed to complete the full process is impacted by many factors like the search space, defined in both the dimensions of code delay and Doppler frequency, and the search strategy. The time required to read the navigation data for the position fix includes a small contribution for achieving frame synchronization and the time to retrieve valid information from the message to calculate the pseudoranges. The read time is a function of the epoch at which the reading of the message begins. According to the proposed method, a statistical approach is used for describing this relationship, considering the reading point as a random variable uniformly distributed over the subframe. The probability density function of the data read time is obtained from the observed occurrences and then the 95% value can be computed from the cumulative distribution function. In the paper several test results using different GNSS signals and the three receiver start conditions are presented and commented.

The work is concluded with some critical considerations underlining which aspects make one signal different from the other with respect to its TTFF performance.

INTRODUCTION

In the current GNSS scenario, thanks to the coming of the European Galileo and other global and regional satellite navigation systems, as well as to the GPS and GLONASS modernization process, new signals are and will be available for the different classes of users to be served. Many aspects of innovation come with these signals, including the use of longer spreading codes, new modulation techniques and new navigation message structures, which make use of channel coding techniques.

In such a wide variety it is essential to define criteria and figures of merit that allow to understand which are the main differences among the signals, in which case the one would perform better than the other, which one would be more suitable for a certain application field and which rather not.

Among the different performance analyses, the estimation of the so called Time-to-First-Fix (TTFF) plays a fundamental role, being this one of the most concrete feedback on the quality of the service that a GNSS gives to the users.

Within this work we propose a method for estimating the TTFF of different GNSS signals with the 95% confidence and present detailed simulation results, obtained applying the method to some GPS and Galileo signals.

DEFINITION OF TTFF

With the expression Time-To-First-Fix we generally refer to the time needed by the receiver to perform the first position fix, starting from the moment it is switched on.

Usually we can distinguish between three different TTFF scenarios, depending on the particular status of the receiver when it is started. We refer to cold, warm or hot start according to the availability and validity of the data required to compute the navigation solution (satellite almanac and ephemeris parameters, send time of the received signal, previously stored PVT solutions). The three cases can be described as follows:

- **Cold Start** No data is stored in the receiver, however the position solution can be calculated by a full sky search without the use of any almanac data. *For the first position fix, clock correction and ephemeris data (CED), together with a GNSS time reference (GST) must be retrieved.*
- **Warm Start** Valid ephemeris and clock corrections are stored in the device and *the receiver just needs to retrieve the GST information from the navigation message.*
- **Hot Start** The warm start conditions apply; in addition, accurate position and clock error are known. *The position solution can be computed without any information from the navigation message.*

Beside the availability of the navigation data, the TTFF performance depends on the amount of the visible satellites and on the strength of the received signals.

All our analyses have been performed under the assumption that the signals are received with high enough C/N_0 (e.g. no bit errors) and that the number of visible satellites is always sufficient to allow the receiver to perform a first position fix within the standard accuracy requirements. Moreover the receiver has to be able to process all the signals coming from the different satellites in parallel, as it commonly happens in nowadays receiver. Under these conditions the TTFF equals the time needed to process one of the signals coming from the different satellites.

In the following sections we present a methodology for the computation of the 95% probability of TTFF; this method could be applied to any GNSS signal.

The approach can be seen as a generalization of [1], where the TTFF is subdivided into different contributions, the value of which can be estimated separately, obtaining the final result as their combination.

CONTRIBUTIONS TO THE TTFF

The single contributions to the TTFF are related to the individual tasks performed by the receiver from the moment it is switched on to the first valid position solution.

Depending on the start condition, the TTFF can be described as follows:

$$TTFF_{cold} = T_{warm-up} + T_{acq} + T_{track} + T_{CED+GST} + T_{PVT} \quad (1)$$

$$TTFF_{warm} = T_{warm-up} + T_{acq} + T_{track} + T_{GST} + T_{PVT} \quad (2)$$

$$TTFF_{hot} = T_{acq} + T_{track} \quad (3)$$

where:

- $T_{warm-up}$: receiver warm-up time
- T_{acq}: acquisition time;
- T_{track}: settling time for code and carrier tracking;
- $T_{CED+GST}$: navigation data read time (CED and GST);
- T_{GST}: time to retrieve the system time reference;
- T_{PVT}: time to compute the navigation solution.

The receiver warm-up time includes all software and hardware initializations that are carried out from the very first moment of switching-on. Obviously it strongly depends on the technology of the considered GNSS receiver. For our purpose we refer to [1], where this time is considered to be around 2 seconds.

The time to compute the navigation solution is mainly due to the initialization of the algorithms for the positioning solution (e.g. Kalman filter or least squares method). Especially for the cold start case where there is no knowledge of the user position, the algorithms are initialized supposing to be in the center of the earth. This could make the T_{PVT} contribution to be a bit longer. A very approximate positioning solution can be available for the warm start, and thus this contribution becomes smaller. Finally, for the hot start case, this time can be considered negligible.

We will now discuss in detail the main contributors to the overall TTFF computation. The theory necessary to compute $T_{acq,}$ T_{track}, $T_{CED+GST}$ and T_{GST} is presented in the following sections.

ACQUISITION TIME

The acquisition time is one of the dominant components of the TTFF. The acquisition process is a detection problem and is usually performed in a navigation receiver by measuring the complex amplitude of the output of the correlator. At this scope a test statistic is defined and compared with a predefined fixed threshold. This threshold indicates whether the signal that we are looking for is present or not. The threshold is set in order to minimize the probability of false alarm and to keep a high probability of detection. As illustrated in [4], during the coherent integration, a number M of Intermediate Frequency (IF) in-phase (I) and quad-phase (Q) prompt correlator samples are summed coherently. After this, the obtained results are squared and added to each other, resulting in the following expression:

$$y_C = \left(\sum_{i=1}^{M} I_i \right)^2 + \left(\sum_{i=1}^{M} Q_i \right)^2 \quad (4)$$

The number M of samples to be summed up in the coherent integration is actually determined by using a coherent integration time T.

For the scope of this paper the further non-coherent summation of the of the y_c of the previous equation will not be considered and therefore the test statistic that will be used for the acquisition process is the one of equation (4). As explained in [4], the signal detection problem is basically a statistical exercise based on a hypothesis test, and defining TH as the test threshold, we have:

- $y_C > TH$ under the hypothesis H_1 (signal present)
- $y_C < TH$ under the hypothesis H_0 (signal not present)

The single cell probability of detection for the threshold TH can be defined as follows:

$$p_d = \int_{TH}^{\infty} p(y_C \mid H_1) dy_C = \int_{TH}^{\infty} \frac{1}{2} e^{-\frac{y_C - \alpha}{2}} I_0\left(\sqrt{\alpha y_C}\right) dy_C \quad (5)$$

where I_0 is the Bessel function and $\alpha = 2T\ C/N_0$ is the post-correlation signal to noise ratio, and similarly the single cell probability of false alarm is follows:

$$p_{fa} = \int_{TH}^{\infty} p(y_C \mid H_0) dy_C = \int_{TH}^{\infty} e^{-y_c} dy_C \quad (6)$$

As well known, the acquisition is performed following a two-dimensional search in frequency and code delay. The elements that need to be defined in order to correctly estimate the acquisition time are the search space and the search strategy.

The search space has to cover the full range of uncertainty of the code delay and carrier Doppler shift. The dimension of this range as well as the resolution of the search has to be accordingly defined. With respect to the code delay search space, the range of the possible offset values depends on the specific code that has to be acquired, while for the Doppler frequency shift search space, this is fixed to be a maximum possible Doppler shift f_d^{MAX}. In order to correctly dimension the frequency search space, the dynamics of both the satellite and of the user need to be taken into account, considering without loss of generality that the receiver oscillator mismatch is negligible. The maximum possible Doppler shift definition is indeed strictly related to the maximum dynamic range according to the following expression:

$$f_d^{MAX} = V_{\max} f_o / c \quad (7)$$

where f_0 is the carrier frequency, defined in Hz, V_{max} is the maximum dynamic range, related to the relative movement between user and satellite, defined in m/s, and c is the speed of light, defined in m/s. Therefore the Doppler search dimension depends on the carrier frequency of the signal to be acquired, on the particular orbital characteristics of the constellation that is transmitting the signal and on the speed of the user that is receiving it. For the simulations a user moving at a velocity of 5 m/s has been considered.

The maximum Doppler frequencies to be searched, for the signals to analyze, have been calculated and are listed in the following table.

Signal	f_d^{MAX} **[Hz]**
Galileo E1-B	4163
Galileo E5a-I	3109
GPS L1 C/A	4893
GPS L1C	4893

Table 1: Maximum Doppler Frequency

Concerning the resolution of the search space, for the code delay dimension a half code chip is normally assumed. With respect to the Doppler shift resolution, a Doppler bin is defined to be the fundamental unit and its width depends mainly on the integration time and can be defined as follows:

$$\delta f = 2/3T \quad (8)$$

As explained in [5], the size of the Doppler frequency bin δf is obtained from the zero crossing point of the sinc function of the Doppler frequency error and therefore results to be inversely proportional to the integration time T. It must be underlined that in this work the coherent integration time for each signal has been considered equal to the inverse of the data rate, and therefore:

Signal	T **[ms]**
Galileo E1-B	4
Galileo E5a-I	10
GPS L1 C/A	20
GPS L1C	10

Table 2: Coherent integration time values

In consequence the search space dimension calculates to:

$$N = N_f N_T = \frac{\Delta f}{\delta f} \frac{\Delta T}{\delta t} \quad (9)$$

where $\Delta f = 2 f_d^{MAX}$ is the range of frequency values to be searched, ΔT is the range of code shift values to be searched and equals the length of the code and δf and δt

are the frequency and code shift bin dimensions respectively.
Under these hypotheses the search space dimensions for the four signals analyzed in this work have been calculated, and the results are reported in the following table.

Signal	N_f	δf [Hz]	N_T	δt [chips]
Galileo E1-B	50	166	8184	0.5
Galileo E5a-I	94	66	20460	0.5
GPS L1 C/A	294	33	2064	0.5
GPS L1C	147	66	20460	0.5

Table 3: Search space dimensions

If some cells are searched in parallel in a multi-correlator receiver, and/or by means of an FFT approach, as it happens in a modern GNSS receiver, the number of correlations that are needed is decreasing. If P_f and P_T are representing the number of frequency and code bins that are searched in parallel, than the total number of parallel correlations that are needed in the acquisition process are:

$$N_p = \frac{N}{P} = \frac{N_f N_T}{P_f P_T} = N_{p_f} N_{p_T} \tag{10}$$

where $P=P_fP_T$ is the total number of bins that are searched in parallel in both code and frequency and $N_p=N_{pf}N_{pT}$ is the total number of parallel correlations that are really contributing to the acquisition time.
In the case of warm and hot start, a reacquisition process is considered. In these cases the search space is reduced with respect to the whole one. The code shift dimension remains unchanged, while the number of Doppler shift to be accounted for will be smaller under these conditions. For the means of this paper the dynamic rate for a signal transmitted at L-band frequencies has been estimated in 1 Hz per second.

Concerning the search strategy, following [6], three main options will be considered:

- Serial search strategy: it consists in serially evaluating the search space cell by cell stopping the acquisition process as soon as the threshold is exceeded for the first time. Details on the serial search strategy can be found in [7].
- Maximum search strategy: in this case the correlation function is evaluated all over the search space and the decision is taken only on the maximum of the search space. Details on the maximum search strategy can be found in [8].
- Hybrid search strategy: being a combination of the previous two, the search space is evaluated row by row (or column by column), and the decision is taken on the maximum of each row (or column). The acquisition process terminates as soon as a maximum in the current row (or column) exceeds the threshold. In such an approach also FFT-based algorithms can be employed. Details on the hybrid search strategy and the FFT search can be found in [9].

As well explained in [6] and [10], the expressions of the probability of detection and probability of false alarm for the acquisition process previously introduced are independent of the search strategy, since they are evaluated on the single cell of the search space. In [6] and [10] the expressions of the so-called system detection and false alarm probabilities are introduced and the corresponding expressions will be used in this work for the evaluation of the acquisition time for the various search strategies. The system detection probabilities for the three search strategies previously introduced are the following:

$$p_{D,Serial} = \frac{1}{N_p} \frac{1-\left[1-p_{fa}\right]^{N_p}}{p_{fa}} p_d \tag{11}$$

$$p_{D,Maximum} = \int_{TH}^{\infty} \left[1-p_{fa}\right]^{N_p-1} p\left(y_C \mid H_1\right) dy_C \tag{12}$$

$$p_{D,Hybrid} = \frac{1}{N_{p_f}} \frac{1-\left[1-p_{fa}\right]^{N_p}}{1-\left[1-p_{fa}\right]^{N_{p_T}}} \int_{TH}^{\infty} \left[1-p_{fa}\right]^{N_{p_T}-1} p\left(y_C \mid H_1\right) dy_C \tag{13}$$

where p_d and p_{fa} are the single cell probabilities of detection and false alarm.
Since, as explained in [10], the acquisition decision is generally taken on the basis of the whole search space, the system probabilities just introduced are extremely important, especially in this analysis that aims at calculating the time needed to perform the acquisition process. These probabilities are defined under the assumptions that the single cell probabilities are verified only on one cell of the search space and that the random cells of a search space are supposed to be statistically independent.
Let us now derive the expression of the acquisition time for the easiest case, represented by the maximum search strategy. In the case of a maximum search, the mean time to sweep the whole search space is given, according to [11], by the following expression:

$$\overline{T}_{SW} = \left(1+K\left(p_{fa}\right)_p\right) T N_p \tag{14}$$

where T is the coherent integration time and N_p is the search space dimension as they have been previously defined, while, as in [11], $(p_{fa})_p$ is the effective false alarm probability that takes into account the fact that more cells are searched in parallel and can be defined as follows:

$$\left(p_{fa}\right)_p = 1-\left(1-p_{fa}\right)^P \tag{15}$$

Moreover, in equation (14) KT is the so-called penalty time, defined in [11] and needed to verify that the false alarm is really a false alarm and not a true lock point. For the simulations in this paper K=3 has been considered.
In the case of a serial search, it has been considered that the mean sweep time is half the one required for a maximum search, since the acquisition process is stopped as soon as the threshold is exceeded and therefore, as said in [6], on average only half of the search space is evaluated.

Using the mentioned definition of mean sweep time, again following [11], the probability of acquisition after n searches of $n\overline{T}_{SW}$ seconds through the search space can be defined as follows:

$$P_{acq}\left(n\overline{T}_{SW}\right)=1-\left(1-P_D\right)^n \qquad (16)$$

where P_D is the system probability of detection for different search strategies. Therefore, if the required probability of acquisition is higher than the system probability of detection, more than one sweep of the search space is needed. By fixing a given probability of acquisition (in the case of this paper 0.95), the corresponding time needed to acquire the signal with that probability can be calculated.

In the simulations performed for this paper, a high number of correlators (30,000) has been considered for all the three search strategies, as common in nowadays navigation receivers. Moreover, a single cell detection probability of 0.9 and a single cell false alarm probability of 10^{-4} have been assumed.
The acquisition time for 95% of confidence has been calculated for four GNSS signals, using the three different search techniques mentioned before; cold, warm and hot start cases have been considered. For the warm and the hot start a reacquisition after 30 minutes and 60 seconds respectively has been chosen. The results of the simulations for the $T_{acq}(95\%)$ are listed in the three following tables for maximum, serial and hybrid search respectively.

Signal	*Cold Start*	*Warm Start*	*Hot Start*
Galileo E1-B	1.11	0.50	0.05
Galileo E5a-I	13.15	7.69	0.57
GPS L1 C/A	8.22	3.05	0.27
GPS L1C	20.65	7.69	0.57

Table 4: $T_{acq}(95\%)$ [s] – Maximum Search

Signal	*Cold Start*	*Warm Start*	*Hot Start*
Galileo E1-B	0.56	0.25	0.02
Galileo E5a-I	6.92	3.97	0.28
GPS L1 C/A	4.18	1.54	0.13
GPS L1C	11.11	3.97	0.29

Table 5: $T_{acq}(95\%)$ [s] – Serial Search

Signal	*Cold Start*	*Warm Start*	*Hot Start*
Galileo E1-B	0.02	0.01	0.01
Galileo E5a-I	0.13	0.13	0.11
GPS L1 C/A	0.14	0.14	0.10
GPS L1C	0.13	0.13	0.11

Table 6: $T_{acq}(95\%)$ [s] – Hybrid Search

TRACKING LOOPS INITIALIZATION

The receiver's tracking loop (PLL, FLL and DLL) require, before entering in their stable region, a transient time which can be estimated by studying their step response. As can be seen in Figure 1, the settling time of PLL and DLL are significantly smaller compared to the time required by the FLL. Obviously these considerations are dependent on the loop bandwidths.

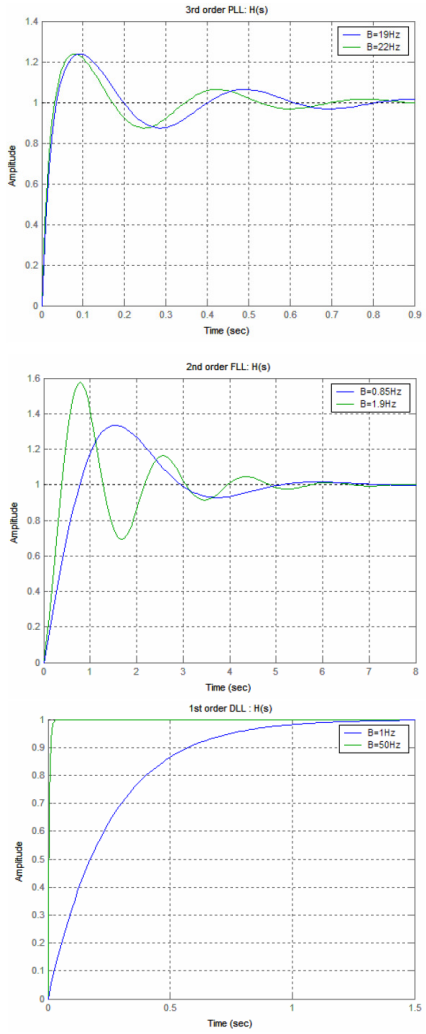

Figure 1: Step response of the tracking loops in a GNSS receiver [2]

Being the FLL settling time in the order of 4 to 5 s (for a B=0.85 Hz), we can refer to these values for our estimate of T_{Track}, as also suggested in [1]. In our analyses we chose the value 4.8 s for the cold and warm start cases, which more or less corresponds to the 95% of the time to reach the stable region. In case of hot start this time contribution reduces significantly and a value of 0.5 s can be assumed.

FRAME SYNCHRONIZATION

In today's navigation messages, the data is arranged in a multi-level structure that, depending on the considered GNSS, is composed of "frames", "subframes", "messages", "pages" and "words".

What is common to all the different messages is that, after retrieving the navigation bits, a sort of validity check should be performed (e.g. Cyclic Redundancy Check).
Considering the amount of information bits to which this check applies, together with the field containing the check bits, we will call "page" the block of navigation symbols obtained by encoding these bits, plus eventually the so called synchronization sequence.
It should be noted that in case of the Galileo I/NAV message, one "page" is a data structure repeating every 1 s. It includes a synchronization field at its front and its information bits are convolutionally encoded and block interleaved. What we call "page" in the framework of this work for generalization, is actually named "word" in the Galileo I/NAV message.
With the expression *frame synchronization* we refer to the search process leading to the identification of the starting point of a valid page. This is generally achieved by reading a known sequence of symbols located at the beginning of each page and called sync word. For example all the Galileo I/NAV message pages begin with the sequence 0101100000.
We define the T_{sync} as the time between the epoch at which the first navigation symbol coming from the tracking loop is available and the epoch of the first successful validity check.
Assuming that there are no bit errors, the worst case, causing the longest waiting time, is when the first retrieved navigation symbol is located at point A in Figure 2, i.e. it is the second bit of the currently processed page.

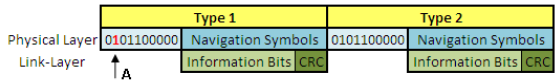

Figure 2: Generic structure of two consecutive pages

In this case, omitting the processing time to compute the CRC which can be considered negligible, T_{sync} is equal to the duration of two pages minus one bit. The relationship between T_{sync} and the symbol rate is given by:

$$T_{sync} = \frac{1}{r_s}\left(2 \cdot L_{Page} - 1\right) \qquad (17)$$

Where L_{page} is the number of navigation symbols in one page and r_s is the symbol rate. From Equation (17) it is clear that an increased symbol rate helps reducing the time needed for the frame synchronization.
A special case can be considered the frame sync procedure of the GPS L1C signal. Its message, called CNAV-2, does not present any sync field, because the frame synchronization should be achieved thanks to a secondary code modulated on the pilot component. This sequence has exactly the same length of one frame (1800 symbols) and was chosen such that the correlation with shorter sequences would also allow synchronization. In [3] it is shown that a sequence of 100 symbols (1 s) would be enough for identifying where the frame starts univocally.
In order to be coherent with the approach used in this work, the values of T_{sync} were computed with the 95% confidence. Table 7 shows the obtained numbers.

Signal	***Frame Sync Time* [s]**
Galileo E1-B	1.95
Galileo E5a-I	1.95
GPS L1 C/A	11.72
GPS L1C	1.00

Table 7: Frame synchronization time of different GPS and Galileo signals

In the next section a detailed description of the methodology used for the computation of the required time to read the data will be presented. Since the synchronization time presented in Table 7 can be included into the data read time, there will be no explicit contribution from the sync time to the TTFF (as can be also seen in equations (1), (2) and (3)).

NAVIGATION DATA READ TIME

In this section we concentrate on the terms $T_{CED+GST}$ and T_{GST}, which represent the time needed by the receiver to retrieve the navigation parameters required for the computation of the pseudoranges to the satellites.
As explained before, this set of parameters depends on the start condition. Without loss of generality we can divide them into two groups: the clock and ephemeris parameters (CED) and the GNSS time (GST) parameters. The former describe the position of the satellite in its orbit and the satellite clock error, while the latter give information about the time that a particular message was sent at and represents an essential reference point for the PRN code ambiguity resolution.
In case of a cold start, both CED and time information are missing, while for a warm start, the availability of a valid CED allows to perform the first position fix just after reading the send time information.

As already mentioned at the beginning, we want to estimate the value of the data read time with the 95% confidence, and this can be obtained from its cumulative distribution function (CDF). Once we have this value, we can add it to the estimates of the other TTFF contributions.
Since the CDF is the integral of the probability density function (PDF), the first step will be to obtain this curve.
Before proceeding with its computation, a brief description of the generic structure of navigation messages is presented.
All data we are interested in is contained, together with other parameters, in the so called navigation message transmitted by the satellites in the form of a long bit sequence. Each GNSS has its own terminology for describing these groups of bits and there are also different logical ways to identify one particular group.
As already explained, within this work we will use the terminology of the European Galileo system (e.g. used for the F/NAV) and call "page" a sequence of bits whose validity is proven by a cyclic redundancy check (CRC) situated at the end each page. The page represents the

smallest block of information where a single bit error would cause the whole block to be considered invalid and therefore discarded.

Another important remark is that, for the validity of the page, it is essential that the whole block is received and decoded: if the reading of the message starts one bit after the beginning of the current page, it will be considered invalid and one has to wait until the next complete page for retrieving useful information.
Pages of different types are transmitted one after each other for the duration of one subframe, which identifies the upper logical group of information.
Due to their importance and urgency and unlike some other parameters (almanac data, differential corrections or other system parameters), the CED and the GST are regularly transmitted within each subframe at a repetition time given by the subframe length in seconds.
Table 8 shows the repetition interval of CED and GST for some GNSS signals.

GNSS	*Signal*	*Navigation Message*	*GST Interval*	*CED Interval*
Galileo	E1-B	I/NAV	15 s	30 s
Galileo	E5a-I	F/NAV	50 s	50 s
GPS	L1 C/A	NAV	6 s	30 s
GPS	L1C	CNAV-2	18 s	18 s

Table 8: Repetition intervals of CED and GST for various GNSS signals

To give an example we take the structure depicted in Figure 3, which is based on the Galileo I/NAV message. A subframe repeating every 30 seconds is shown. The green pages contain CED, while the grey ones contain the system time information. One should note that, while all the four green pages should be retrieved for having valid CED, the GST could be retrieved either from page 5 or 6 without any distinction.

Elapsed Time [s]	*Page Type*	*Elapsed Time [s]*	*Page Type*
1	Page 2 – CED (2/4)	16	Page 11
2		17	Page 16
3	Page 4 – CED (4/4)	18	
4		19	Page 15
5	Page 6 – GST	20	
6		21	Page 1 – CED (1/4)
7	Page 7/9	22	
8		23	Page 3 – CED (3/4)
9	Page 8/10	24	
10		25	Page 5 - GST
11	Page 12	26	
12		27	Spare
13	Page 14	28	
14		29	Spare
15	Page 11	30	

Figure 3: Example structure of a navigation message subframe (Galileo I/NAV)

Once analyzed the structure, the first thing to do is to make a table of the time needed to read both CED and GST considering all the possible points where the reading process can start.
Depending on whether the current page contains the parameters required for the first position fix or not, we consider also the cases where the reading point is immediately after the beginning of the page. For a page starting at the time 0, such epoch (implying the loss of the first bits) will be indicated as 0^+.
Table 9 shows the $T_{CED+GST}$ values referring to the subframe structure of the Galileo I/NAV message; as we can see, after 30 seconds the time values repeat as for the previous subframe.

Reading Epoch	$T_{CED+GST}$ [s]	$T_{CED+GST}$ [s]	*Reading Epoch*
0	24	16	18
0^+	32	17	17
1	31	18	16
2	30	19	15
2^+	32	20	14
3	31	20^+	32
4	30	21	31
5	29	22	30
6	28	22^+	32
7	27	23	31
8	26	24	30
9	25	25	29
10	24	26	28
11	23	27	27
12	22	28	26
13	21	29	25
14	20	30	24
15	19	31	32

Table 9: Time to get navigation data from the Galileo I/NAV message for different reading epochs

These values can be plotted to have a rough idea of the reading epoch vs. required reading time characteristics (Figure 4).

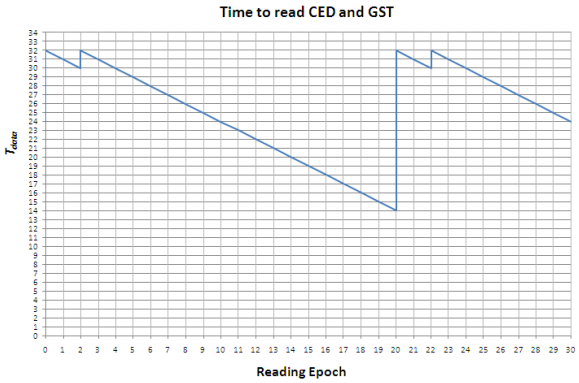

Figure 4: Time to read CED and GST from the Galileo I/NAV message as a function of the reading epochs

As we can see, the read time changes as descending straight lines presenting discontinuities where the reading epoch is located just after the beginning of a page of interest ($t = 0^+$, $t = 2^+$, $t = 20^+$ and $t = 22^+$).
The function can be described as follows:

$$\begin{cases} x(t) = 24 & t = 0 \\ x(t) = -t + 32 & 0 < t \le 2 \\ x(t) = -t + 34 & 2 < t \le 20 \\ x(t) = -t + 52 & 20 < t \le 22 \\ x(t) = -t + 54 & 22 < t \le 30 \end{cases} \quad (18)$$

We will now proceed in our analysis to obtain the probability density function *f(t)* of $T_{CED+GST}$. We assume that the entry point in the subframe is uniformly distributed over its length in seconds and we count for the frequency with which each possible $T_{CED+GST}$ is observed. The fact that the searched curve should integrate to 1 allows computing the probability values by normalizing the occurrences. The results are shown in Figure 5.

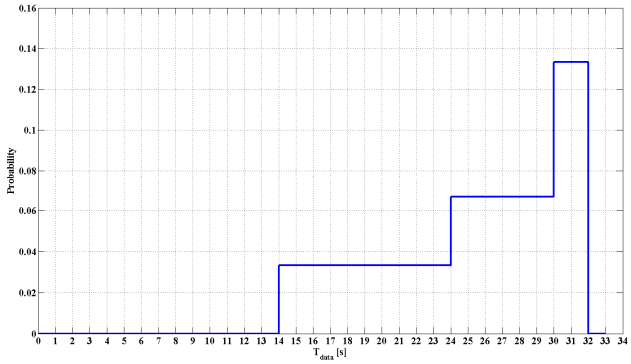

Figure 5: Probability density function of the time to read the Galileo I/NAV message

The mathematical form of the PDF is given by:

$$f(t) = \begin{cases} \frac{1}{30} & 14 \le t \le 24 \\ \frac{1}{15} & 24 \le t \le 30 \\ \frac{2}{15} & 30 \le t \le 32 \\ 0 & \text{elsewhere} \end{cases} \quad (19)$$

At this point the 95% probability can be obtained from the following relationship:

$$F(T_{CED+GST}) = \int_{-\infty}^{T_{CED+GST}} f(t)\mathrm{dt} = 0.95 \quad (20)$$

Still referring to our example, solving (20) by iteration, we obtain $T_{CED+GST}$ = 31.63 s as final result.

Summarizing, this value represents, with 95% confidence, the time needed by the receiver to retrieve CED and GST parameters, from the Galileo I/NAV message. We remind that these parameters are necessary for the first position fix, just in case of a cold start.

For the warm start case, just GST needs to be retrieved; the values for the time required to read this data is shown in Table 10:

Reading Epoch	T_{GST} [s]	*Reading Epoch*	T_{GST} [s]
0	6	16	10
1	5	17	9
2	4	18	8
3	3	19	7
4	2	20	6
4^+	22	21	5
5	21	22	4
6	20	23	6
7	19	24	2
8	18	24^+	12
9	17	25	11
10	16	26	10
11	15	27	9
12	14	28	8
13	13	29	7
14	12	30	6
15	11	31	5

Table 10: Galileo I/NAV. Time to get the system time reference for different reading epochs

Accordingly, the plot of the probability density function changes, as presented in Figure 6.

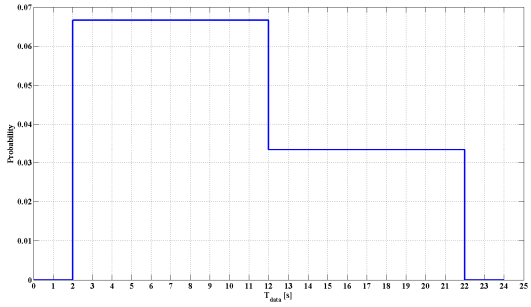

Figure 6: PDF of the time to read the GST from the Galileo I/NAV message

Also for the warm start case the 95% probability can be obtained by iteration from the cumulative distribution function resulting in T_{GST} = 20.60 s.

All these estimates concerning the data read time must be added to the other contributions in order to come up with the overall TTFF estimate.

We applied this approach to different GNSS signals estimating for $T_{CED+GST}$ and T_{GST} the values reported in Table 11.

System and Signal	*Message*	$T_{CED+GST}$ [s] *95% (Cold Start)*	T_{GST} [s] *95% (Warm Start)*
Galileo E1-B	I/NAV	31.6	20.6
Galileo E5a-I	F/NAV	59.2	37.5
GPS L1 C/A	NAV	35.5	11.7
GPS L1C	CNAV-2	17.6	17.6

Table 11 : Estimates of the navigation data read time for different GNSS signals.

Please note that for the hot start case, according to (3), there is no contribution of the data read time.

SIMULATION RESULTS

According to Equations (1), (2) and (3) and substituting the estimates obtained following the approach explained in the previous sections, we come to the final results reported in Table 12, Table 13 and Table 14 for cold, warm and hot start respectively. Please note that the time contributions for the acquisition refer to the Maximum Search strategy.

System and Signal	$T_{warm-up}$ [s]	T_{acq} [s]	T_{track} [s]	$T_{CED+GST}$ [s]	T_{PVT} [s]	$TTFF_{cold}$ [s]
Galileo E1-B	2.0	1.1	4.8	31.6	2.0	41.5
Galileo E5a-I	2.0	13.1	4.8	59.2	2.0	81.1
GPS L1 C/A	2.0	8.2	4.8	35.5	2.0	52.5
GPS L1C	2.0	20.7	4.8	17.6	2.0	47.1

Table 12 : Time-to-First-Fix estimates for the receiver cold start.

System and Signal	$T_{warm-up}$ [s]	T_{acq} [s]	T_{track} [s]	T_{GST} [s]	T_{PVT} [s]	$TTFF_{warm}$ [s]
Galileo E1-B	2.0	0.50	4.8	20.6	2.0	29.9
Galileo E5a-I	2.0	7.69	4.8	37.5	2.0	54.0
GPS L1 C/A	2.0	3.05	4.8	11.7	2.0	23.6
GPS L1C	2.0	7.69	4.8	17.6	2.0	34.1

Table 13 : Time-to-First-Fix estimates for the receiver warm start.

System and Signal	T_{acq} [s]	T_{track} [s]	$TTFF_{hot}$ [s]
Galileo E1-B	0.05	0.5	0.55
Galileo E5a-I	0.57	0.5	1.07
GPS L1 C/A	0.27	0.5	0.77
GPS L1C	0.57	0.5	1.07

Table 14 : Time-to-First-Fix estimates for the receiver hot start.

As can be seen in the previous tables, the Galileo E1-B signal shows the best TTFF performance for the cold and the hot start cases, while for the warm start the GPS L1 C/A code outperforms all other signals.

The very low data rate of the Galileo E5a-I signal results in a quite long data read time and, as a consequence, its TTFF performance is the worst for the cold start case.

Looking at the results obtained for the GPS L1C signal, we can see how the poor performance in terms of acquisition time due to the long coherent integration time and to the length of the PRN codes, is counterbalanced by a very short data read time. The GPS L1C signal is indeed presenting the shortest data read time because of its particular navigation message structure allowing for a very short ephemeris repetition time.

CONCLUSION

A methodology for the computation of the TTFF for different Galileo and GPS signals has been presented distinguishing the cases of cold, warm and hot receiver start. The main contributions to the TTFF have been discussed and simulated considering also different acquisition search strategies.

Since the acquisition time contribution can be highly decreased by employing new algorithms and technologies, the key factor for a good TTFF performance turns out to be the design of the navigation message structure

As mentioned before, all the TTFF estimates have been obtained under the assumption that the signals were received with a high enough carrier to noise ratio density, and thus with no bit errors.

Further studies are being carried out to analyze the behavior of the Time-to-First-Fix in low C/N_0 environments and the results will be published in [12].

The proposed method could be easily implemented in GNSS performance simulation tools and also be adopted in several GNSS theoretical studies, especially those regarding new generation systems.

REFERENCES

[1] Holmes J.K., Morgan N. and Dafesh P., *A Theoretical Approach to Determining the 95% Probability of TTFF for the P(Y) Code Utilizing Active Code Acquisition*, ION GNSS 2006, Fort Worth, Texas, USA, 26-29 September 2006

[2] Won J.-H., *Studies on the Software-Based GPS Receiver and Navigation Algorithms*, PhD Dissertation, Ajou University, December 2004

[3] Rushanan J. J., *The Spreading and Overlay codes for the L1C Signal,* Journal Navigation ISSN 0028-1522 CODEN NAVIB3

[4] Van Dierendonck A. J., *GPS Receivers*, in *Global Positioning System: Theory and Applications. Vol. I*, Edited by B.W. Parkinson and J. J. Spilker Jr., Stanford University, USA, 1995

[5] Won J.H., Eissfeller B., Lankl B., Schmitz-Peiffer A., Colzi E., *C-Band User Terminal Concepts and Acquisition Performance Analysis for European GNSS Evolution Programme*, ION GNSS 2008, Savannah, GA, USA, September 2008

[6] D. Borio, L. Camoriano, L. Lo Presti, *Impact of the Acquisition Searching Strategy on the Detection and False Alarm Probabilities in a CDMA Receiver*, IEEE/ION PLANS 2006, San Diego, CA, USA, 25-27 April 2006

[7] A. Polydoros, C.L. Weber, *A unified Approach to Serial Search Spread-Spectrum Code Acquisition* – Part I: General Theory, IEEE Transactions on Communications, Vol COM-32, No. 5, May 1984

[8] G.E. Corazza, *On the MAX/TC Criterion for Code Acquisition and Its Application to DS_SSMA Systems*, IEEE Transactions on Communications, Vol. 44, No.9, Sept. 1996

[9] H. Mathis, P. Flammant, A. Thiel, *An Analythic Way to Optimize the Detector of a Post-Correlation FFT Acquisition Algorithm*, ION GPS/GNSS 2003, Portland, OR, USA, 9-12 September 2003

[10] Borio D., *A Statistical Theory for GNSS Signal Acquisition*, Doctoral Thesis, Politecnico di Torino, Italy, March 2008

[11] Holmes, J.K., *Spread Spectrum Systems for GNSS and Wireless Communications,* Artech House, 2007

[12] Paonni M., Anghileri M., Ávila-Rodríguez J.A., Wallner S., Eissfeller B., *Performance Assessment of GNSS Signals in Terms of Time to First Fix for Cold, Warm and Hot Start*, Proceedings of the ION ITM 2010, 25-27 January, San Diego, CA, USA